nature physics

SUPPLEMENTARY INFORMATION

DOI: 10.1038/NPHYS3048

One-dimensional topological edge states of bismuth bilayers

Ilya K. Drozdov[1*], A. Alexandradinata[1*], Sangjun Jeon[1], Stevan Nadj-Perge[1], Huiwen Ji[2], R. J. Cava[2], B. A. Bernevig[1], and Ali Yazdani[1]

[1]*Joseph Henry Laboratories & Department of Physics, Princeton University, Princeton, New Jersey 08544, USA*

[2]*Department of Chemistry, Princeton University, Princeton, New Jersey 08544, USA*

Section I. Edge geometries of supported Bi-bilayers

The three simple types of edges of a honeycomb lattice that are typically considered in the context of graphene are zigzag, armchair and Klein (also known as "bearded") edges (Fig S1)

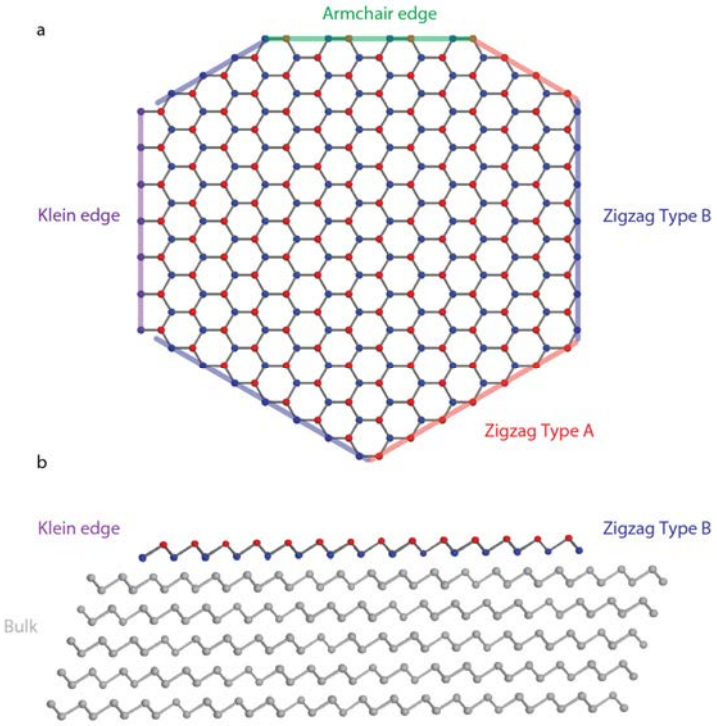

Fig. S1. Different structural types Bi-bilayer edges. a, Top view on the topmost layer of Bi rhombohedral crystal structure terminated with different types of edge geometries. **b,** Side view showing relative orientation of the Klein and Type B edges with the bulk atoms.

When considering a Bi-bilayer in isolation, due to odd number of band inversions one is expected to obtain topological edge states on all types of edges (see e.g. ref. S1 for a calculation of edge states in zigzag and armchair geometries). As an example of the strong topological protection of the edge states of a freestanding Bi-bilayer one can envision a though experiment in which a Type A zigzag edge is transformed into a Klein edge by adding an additional row of Bi atoms (nonmagnetic yet strong perturbation), which would result in one type of topological edge state evolving into another one.

DOI: 10.1038/NPHYS3048

However, when considering a supported bilayer, Klein edges are expected to get strongly hybridized with bulk. The reason being that the outer row of atoms on both edges has direct hoppings to the substrate and thus is expected to delocalize, similar to the case of type B zigzag edge that we consider in detail in the following section. We note, however, that since Type A and B zigzag edges are oriented either 120° or 180° with respect to each other it is impossible to transform a type A edge into type B edge by simply adding an additional row of atoms.

Section II. Hybridization of Type A and B Edges with the Substrate

To compare the hybridization of the two different types of zigzag edges with the substrate we performed a transfer matrix calculation based on the Liu-Allen tight-binding model.[S2] A Bi bilayer ribbon was terminated by two different types of zigzag edges. The 50-unit-cell wide ribbon was placed on top of a 100-unit-cell wide Bi substrate (Fig. S2a). Periodic boundary conditions were imposed along the Y direction, thus momentum along the edge is conserved. The bulk extends semi-infinitely in the –Z direction. In the transfer-matrix method we match the evanescent eigenfunctions of the Hamiltonian to the boundary conditions imposed by the Bi bilayer ribbon. [S2, S3] These evanescent solutions are non-Bloch states with energies within the gap; these solutions decay exponentially in the –Z direction. The calculation reveals two energetically-distinct modes within the gap, and their wavefunctions are localized to type-A and type-B edges respectively (Fig. S2b). The weight of the edge state on the outermost row of atoms is plotted as a function of the conserved momentum along the edge (Fig. S2c) showing that the type-A edge states are more robust against hybridization with the bulk and surface states than those of type-B edge.

Qualitatively this result can be understood by considering the number of bonds connecting the edges to the bulk. The type-B edge has direct hoppings to the substrate which leads to stronger hybridization of the 1D edge mode with the 3D bulk continuum and results in delocalization. On the other hand, the type-A edge has less bonds with the substrate and thus mimics the edge of a freestanding Bi bilayer.

While the above calculation sufficiently demonstrates the difference in hybridization of the two types of edges, it is known that the Liu-Allen tight-binding model cannot quantitatively reproduce the surface state dispersion.[S5] To quantitatively support our claims, we compare our results together with existing fully-relativistic first-principles calculations in ref. S6, where narrow Bi nanoribbons placed on top of a strained bilayer were investigated. Even though the details of the simulation geometry do not exactly match our experiment (which corresponds to larger Bi islands coupled to a macroscopically large substrate), the calculation of ref. S6 nevertheless predicts the same salient properties of the edge modes as described in the main text, namely: (i) robustness of type-A edge states to hybridization with the substrate, (ii) their localization to within a few unit cells from the edge of the terrace, and (iii) the hole-like singularity E_2 in the dispersion.

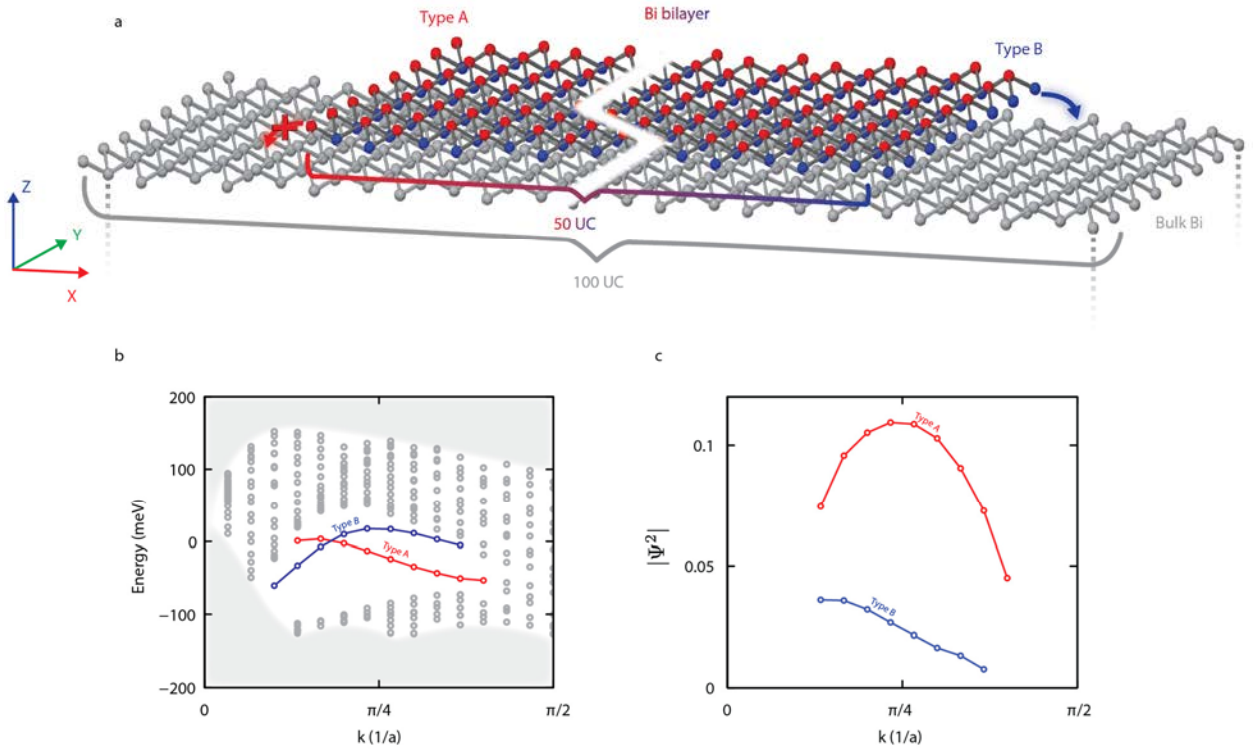

Fig. S2. Hybridization of type A and B edges to the bulk Bi substrate. a, The simulation geometry is schematically illustrated. The top atomic layer of the Bi flake are colored red, while the next-to-top layer is colored blue; the underlying Bi substrate is colored grey and extend semi-infinitely in the –Z direction. **b,** Dispersion of surface states, as calculated from the transfer-matrix method with the illustrated geometry. Red (blue) circles correspond to edge states which are localized at the type-A (-B) edge. Grey circles correspond to 2D surface states; the shaded region corresponds to a continuum of 3D bulk states. **c,** Red plot: weights of the type-A edge states, on the outermost atomic row of type A (the left-most, red-colored row in **a**). The weights are plotted as a function of momentum along the edge. Blue plot: weights of type-B edge states, on the outermost atomic row of type B (the right-most, blue-colored row in **a**).

For illustration, we have reproduced some results from Ref. S5 in Fig. S3. In Fig. S3a, we point out that only a subset of the type-A edge mode lies within the energy gap of the Bi (111) surface continuum. We expect that only this subset is robust against hybridization with the substrate of our experiment; the type-B edge mode lies within the surface continuum and is expected to delocalize. To further support this hypothesis, we have also reproduced in Fig. S3b the real-space probability distributions of both types of edge states. Evidently, the type-B edge state extends deeper into the single-bilayer substrate, and is expected to eventually delocalize for thicker substrates. The results of Fig. S3b compare favorably with our theoretical predictions in Fig. S2c.

DOI: 10.1038/NPHYS3048

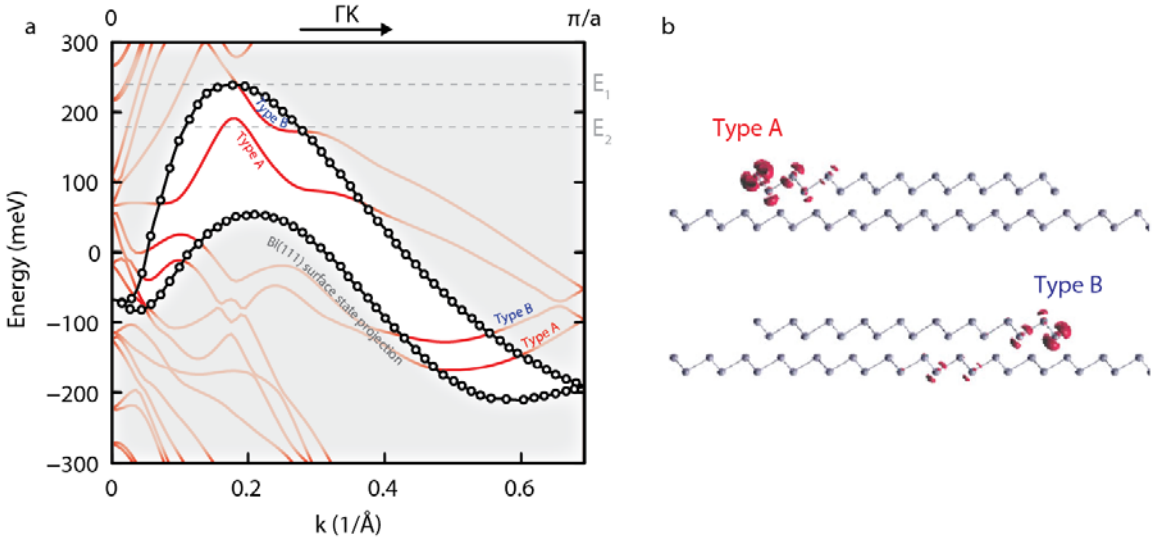

Fig. S3. Comparison to *ab initio* calculations of Bi nanoribbons placed on top tensile-strained Bi BL. a, Result from ref. S5 for the two edge modes of a zig-zag edged Bi BL nanoribbon placed on top of Bi BL on Si(111) are plotted in red. Points are obtained by projecting the result of *ab initio* calculation of the surface state dispersion[S7] onto the 1D BZ of the zigzag edge. Grey region schematically represents the projected Bi(111) surface state continuum on the direction parallel to the edge state (same as in Fig. 4 in the main text). Only a subset of edge modes residing within the gap is expected to survive hybridization with the bulk electronic structure. **b,** Wavefunction weight distribution on the two types of edges for the states at momentum 4π/10a reproduced from ref. S6.

Section III. Van-Hove Singularities in the Point Spectra & Lifetime of 1D states

In our experiments, we have identified two peaks in the point spectra as arising from two different types of van Hove singularities.[S8] Singularities in the density of states (DOS) typically arise in the vicinity of critical points of the band structure. The functional dependence of the DOS in the vicinity of such critical point depends both on the dispersion of the states, as well as on dimensionality of the system. For example, the inverse-square-root dependence as a function of energy DOS $\propto 1/\sqrt{(E_0-E)}$ is characteristic of 1D parabolic dispersion with band maximum occurring at E_0.

The point spectrum away from the step edges on Bi(111) surface in Fig. 1c displays a prominent peak at E_1=213meV, which is identified with a Lifshitz transition in the Bi(111) surface state dispersion (Fig S3a). This transition is a change in the topology of the constant energy contours (CECs) from Fig. S4b to Fig. S4c, and the critical point is a saddlepoint in the 2D dispersion. The DOS is expected to diverge logarithmically at a saddlepoint, thus the DOS near E_1 was fitted with the formula $a + b \log |E-E_1|$.

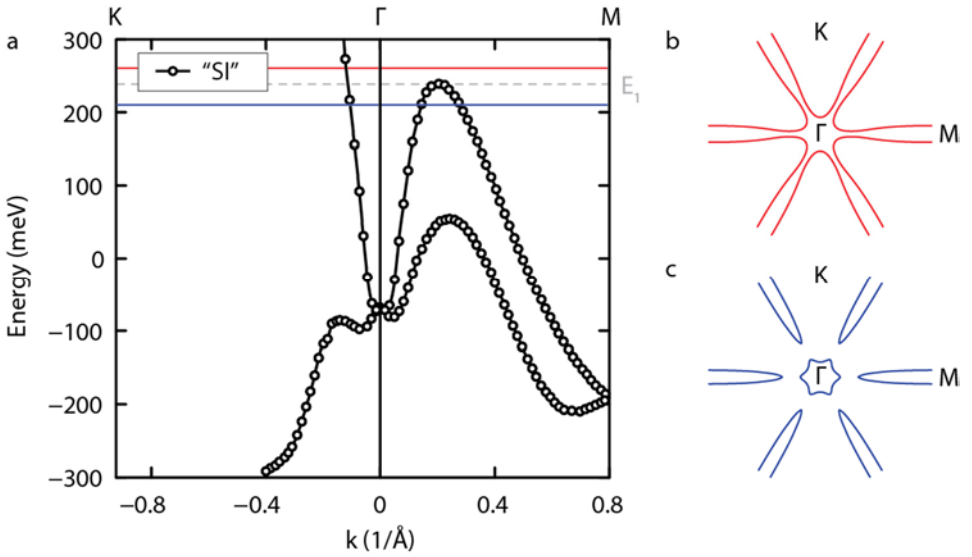

Fig. S4. Bi(111) surface state dispersion. a, The results of *ab initio* Bi(111) surface state calculations are plotted along the high-symmetry directions in the 2D BZ (data reproduced from ref. S7). **b, c** Schematic of the two different CEC topologies of the Bi(111) surface state above and below E_1. The schematics were drawn based on the results reported in ref. S9 for a 10BL calculation.

In contrast, the point spectra on type-A edges show an asymmetric peak around E_2=183meV, which does not correspond to any critical points in the surface states' band structure. The spectrum around E_2 is fitted by a + b/sqrt(E_2-E) function with a small Γ=6meV imaginary component to energy, which represents all the experimental as well as intrinsic energy broadening of our spectroscopic measurements of these 1D states. The resulting fit is plotted as red dashed line in Fig 1c. A large portion of the observed broadening is experimental, since it should consist of 1.3meV (3.5k_BT) of thermal broadening at T=4K and broadening due to finite excitation (3mV RMS), resulting in a total experimental resolution of about 4.5meV. Remarkably, the observed broadening is far smaller than observed before in any type of surface or edge state at energies so far from away from the chemical potential (in this case 200meV). Usually at such energies electron-electron scattering would render electronic states broadened even if they were not coupled to any other states such as bulk states. We can for example contrast this broadening to 50meV broadening of 2D topological surface states of Sb measured by STM[S10]. In contrast, the edge states of Bi exhibit much longer quasiparticle lifetimes, even despite the presence of a conducting substrate.

Section IV. Phenomenological Model of the Topological 1D Edge States

In order to compare experimental data with the predicted QSH edge state of a freestanding Bi bilayer, we employ a Liu-Allen tight-binding model, which we modify with a self-consistent Hartree term to account for Coulomb screening along the edge[S11]. By fitting just a single parameter (the Hubbard on-site energy) we can match the hole-like singularity of the calculated edge mode (inset Fig. 4a) to the experimentally observed hole-like singularity at E_2=183meV (Fig. 1c).

This simple model, matching rather well with the experimental data, also captures the essential physics expected from QSH edge states: (i) the odd number of

DOI: 10.1038/NPHYS3048

left- (right-) movers at Fermi level (ii) absence of backscattering between the time-reversed states (iii) momentum-dependent penetration depth of the edge states[S1]. Specifically with regard to Bismuth, the model produces a hole-like parabolic dispersion that is consistent with our experiment. To compare with QPI data, we compute the overlap of wavefunctions at equal energies and different momenta. Away from the parabolic maximum, the overlap diminishes with increasing momentum separation (Fig. 4A, main panel), as is consistent with experimental data (vanishing intensity of q_1 mode as a function of increasing momentum transfer in Fig. 3).

In Fig. S4b the spin expectation values for a freestanding bilayer model are plotted for the top branch of the edge dispersion (Fig. S4a). The degree of spin polarization monotonically depends on the momentum along the edge. At the highest momenta, the degree of spin polarization is comparable to that of the Bi(111) surface states.[S12]

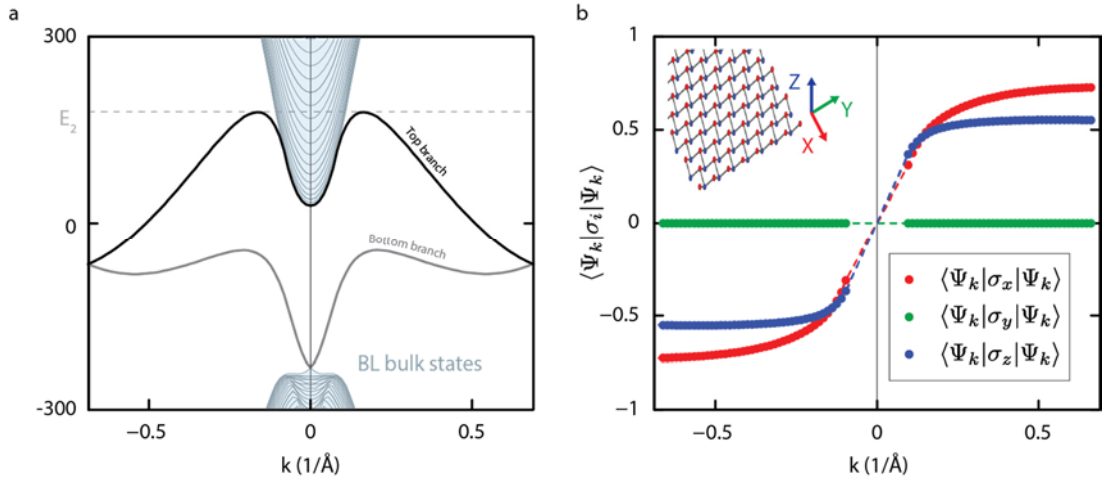

Fig. S4. Dispersion and spin texture in a freestanding bilayer model. a, Dispersion of the zigzag edge state of a freestanding Bi BL. **b,** Spin expectation values for the top branch of the zigzag edge state dispersion are plotted as a function of momentum along the edge. Inset shows the orientation of the coordinate basis with respect to the edge.

Section V. Probing 2D Quasiparticle Interference on the (111) Surface of Bi

Due to energy overlap between the semi-metallic surface state of Bi (111) and the 1D edge state band it is important to reliably separate the 1D edge signatures from the 2D surface state contribution. For this purpose we have experimentally studied surface state 2D quasiparticle interference away from the step edges. Iron adatoms acting as point-like scatterers were deposited *in situ* on a clean (111) surface of Bi away from the edges. 2D Fourier transforms of real space conductance maps at different energies (Fig. S5a) reveal the elastic scattering processes allowed by spin-selection rules[S13]. Fig. S5b shows the energy-momentum dispersion of the QPI modes nested along the two high-symmetry (ΓM and ΓK) directions in the 2D BZ in the same energy range in which the 1d spectroscopic linecuts (in Fig. 2 and Fig. 3) were acquired.

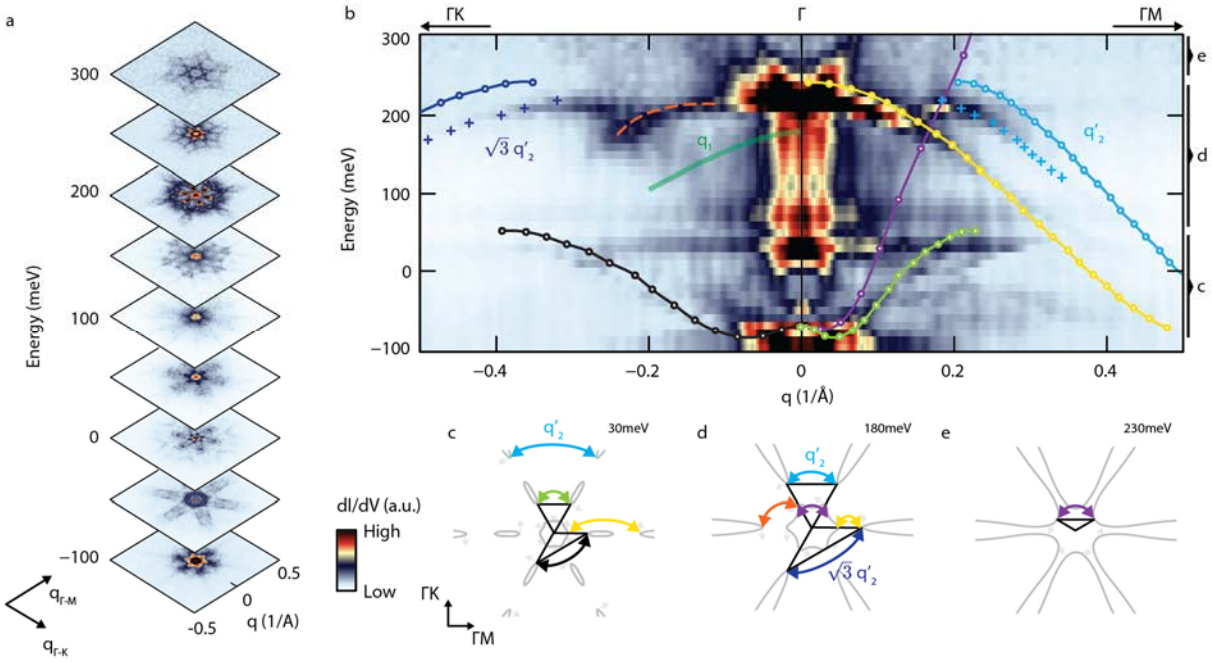

Fig. S5. Bi (111) surface state quasiparticle interference measurements. **a,** 2d Fourier transform of real space conductance maps at few representative energies **b,** QPI branches nested along the Γ-K and Γ-M directions. Momentum differences for the QPI modes obtained from *ab initio* bandstructure[S7] (solid lines and circles) are plotted on top of experimental data. Crosses mark the experimental dispersion of q'_2 mode used for comparison with 1D spectroscopic data in the following. Green guide to the eye marks the 1D edge state dispersion obtained from experiment (Fig. 3). **c-e,** Schematic CECs of three representative topologies are plotted in grey. The schematics were drawn based on the results reported in ref. S9 for a 10BL calculation. Light grey arrows schematically represent the spin texture of the surface state. Colored arrows correspond to different scattering processes allowed by spin selection rules. Color coding of scattering processes is consistent across panels b-e.

The resulting experimental QPI dispersion can be compared to the *ab initio* band structure calculations from ref. S7. By considering CECs and associated spin texture (Fig. S5c-e), nested q-wavevectors allowed by spin selection rules can be identified (arrows in Fig. S5c-e). The corresponding momentum differences are calculated from the theoretical surface band dispersion. The nested scattering wavevectors are approximated by the momentum differences between the tips of the pockets and are plotted on top of experimental data for direct comparison (circles and solid lines in Fig. S5b). The resulting dispersion branches capture well the overall shape of the experimental QPI features with some minor quantitative discrepancy most likely present either due to surface band bending effect or due to slight tip-sample workfunction mismatch.

Finally, a guide to the eye corresponding to the experimental 1D edge state dispersion (obtained from Fig. 3) is plotted on top of surface state 2D QPI showing that no features of 2D QPI nested along ΓK can be attributed to the 1D edge state dispersion described in the main text.

DOI: 10.1038/NPHYS3048

Section VI. Projection of the 2D QPI on 1D Spectroscopic Linecuts

To explain the q_2 feature observed in Fig. 3 we consider the projection of the surface QPI modes on the direction of the edge. This measurement is performed in a geometrical configuration shown in Fig. S6a in which surrounding step edge geometry acts an interferometer for the 2D surface states[S10]. Likewise, the surface state QPI that is nested not necessarily along the direction of the edge is projected on the direction of the 1D measurement resulting in a projected feature corresponding to q_2 (Fig. S6b). Note that this mode does not smoothly connect to the singularity attributed to the 1D edge state. To prove that this mode is indeed originating from the surface state bands we project the experimental dispersion of the surface state intervalley scattering QPI branch (see supplementary section IV, blue crosses in Fig. S5b) on the direction of the measurement (Fig. S5b) which establishes a good agreement between the two independent measurements and confirms the identification of the q_2 feature.

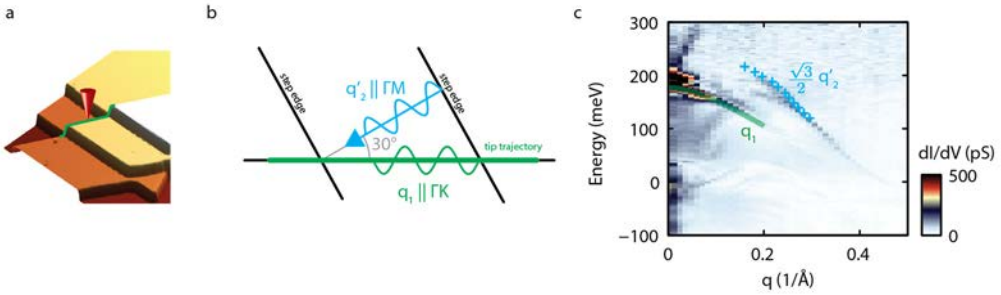

Fig. S6. Surface state QPI projection. a, A topographic image of a type-A edge and its surroundings. Green line schematically shows the tip trajectory corresponding to the spectroscopic linecut presented in Fig 2c. **b**, Schematic illustration of how surface state intervalley q_2 mode trapped between two parallel step edges gets projected onto the direction of the measurement **c,** Fourier transform from Fig. 3 superimposed with projected experimental dispersion of q_2 mode. Blue crosses corresponding to q'_2 surface state mode are derived from 2d QPI experiment (Fig. S5b) and are projected on the direction of the step edge with a geometric √(3)/2 factor. Green guide to the eye marks the 1D edge state dispersion.

Supplementary references

S1. Wada, M., Murakami, S., Freimuth, F. & Bihlmayer, G. Localized edge states in two-dimensional topological insulators: Ultrathin Bi films. *Phys. Rev. B* **83,** 121310 (2011).

S2. Liu, Y. & Allen, R. E. Electronic structure of the semimetals Bi and Sb. *Phys. Rev. B* **52,** 1566–1577 (1995).

S3. Lee, D. H. & Joannopoulos, J. D. Simple scheme for surface-band calculations. I. *Phys. Rev. B* **23,** 4988–4996 (1981).

S4. Heine, V. On the General Theory of Surface States and Scattering of Electrons in Solids. *Proc. Phys. Soc.* **81,** 300 (1963).

S5. Teo, J., Fu, L. & Kane, C. Surface states and topological invariants in three-dimensional topological insulators: Application to Bi1−xSbx. *Phys. Rev. B* **78,** 45426 (2008).

S6. Kotaka, H., Ishii, F., Saito, M., Nagao, T. & Yaginuma, S. Edge States of Bi Nanoribbons on Bi Substrates: First-Principles Density Functional Study. *Jpn. J. Appl. Phys.* **51,** 025201 (2012).

S7. Koroteev, Y. *et al.* Strong Spin-Orbit Splitting on Bi Surfaces. *Phys. Rev. Lett.* **93,** 46403 (2004).

S8. Van Hove, L. The Occurrence of Singularities in the Elastic Frequency Distribution of a Crystal. *Phys. Rev.* **89,** 1189–1193 (1953).

S9. Cottin, M. C. *et al.* Interplay between Forward and Backward Scattering of Spin – Orbit Split Surface States of Bi(111). (2013).

S10. Seo, J. *et al.* Transmission of topological surface states through surface barriers. *Nature* **466,** 343–346 (2010).

S11. Vanderbilt, D. & Louie, S. G. Total energies of diamond (111) surface reconstructions by a linear combination of atomic orbitals method. *Phys. Rev. B* **30,** 6118–6130 (1984).

S12. Hofmann, P. The surfaces of bismuth: Structural and electronic properties. *Prog. Surf. Sci.* **81,** 191–245 (2006).

S13. Roushan, P. *et al.* Topological surface states protected from backscattering by chiral spin texture. *Nature* **460,** 1106–1109 (2009).